Investigation of facet-dependent non-polar growth rates and composition of InGaN for core-shell LEDs

Ionut Girgel[a], Paul R. Edwards[b], Emmanuel Le Boulbar[a], Pierre-Marie Coulon[a], Suman-Lata Sahonta[c], Duncan W. E. Allsopp[a], Robert W. Martin[b], Colin J. Humphreys[c], Philip A. Shields[a]

[a]Department of Electronic and Electrical Engineering, University of Bath, Bath, U.K., BA2 7AY;
[b]Department of Physics, SUPA, University of Strathclyde, Glasgow, U.K., G4 0NG
[c]Department of Materials Science and Metallurgy, University of Cambridge, Cambridge, U.K., CB3 0FS

Abstract. Core-shell InGaN/GaN structures are attractive as light emitters due to the non-polar facets that result from cores oriented in the [0001] c-direction. These facets do not suffer from the quantum-confined Stark effect that limits the thickness of quantum wells and thus efficiency in conventional light-emitting devices. Understanding InGaN growth on these sub-micron 3D structures is important to optimize performance. In this work the influence of reactor parameters was determined and compared. GaN nanowires with both {11-20} a-plane and {10-10} m-plane non-polar facets were prepared to investigate the impact of Metal Organic Vapor Phase Epitaxy (MOVPE) reactor parameters on the characteristics of a thick over-grown InGaN shell. The morphology and optical emission properties of the InGaN layers were investigated by scanning electron microscopy (SEM), transmission electron microscopy (TEM) and cathodoluminescence (CL) hyperspectral imaging. The study reveals that pressure has an important impact on the InN mole fraction on the {10-10} m-plane facets, even at a reduced growth rate. The sample grown at 750°C and 100 mbar had a homogeneous InN mole fraction of 25% on the {10-10} facets of the nanowires. This work demonstrates that homogeneous InGaN/GaN core-shell structures with thick InGaN layers can be grown.

Keywords: core-shell, InGaN, *m*-plane, *a*-plane, non-polar, cathodoluminescence, nanowires

Address all correspondence to: Philip Shields, University of Bath, Department of Electronic and Electrical Engineering, Claverton Down, Bath, UK, BA2 7AY; Tel: +44 1225-386309; E-mail: p.shields@bath.ac.uk

1 Introduction

Most commercial blue LEDs use InGaN/GaN quantum wells in the active region, grown in the [0001] direction, i.e. parallel to the c-plane. These have inherent limitations due to built-in electric fields along the [0001] direction which lead to reduced electron-hole overlap in the active quantum wells (QWs) as a result of the quantum-confined Stark effect[1] (QCSE).

Avoiding QCSE in polar materials normally requires the QWs to be grown perpendicular to the polar axis; on either the non-polar {11-20} and {10-10} planes in wurtzite materials. Another option in the III-nitrides is to grow InGaN quantum wells on semi-polar crystallographic planes, in particular planes oriented at or close to an angle of ~45° to the polar axis. However growth of

III-nitrides on such non-polar and semi-polar planes is less mature than for the (0001) plane, with {10-10} growth typically requiring bulk substrates to avoid high levels of stacking fault defects [2].

In this respect core-shell[3,4,5,3] InGaN/GaN nanowires (NWs) are of considerable interest due to their large surface area of non-polar planes or facets with lower number of defects[6], the potential for high surface to volume ratio[7], and not being subject to detrimental QCSE. These reasons provide a strong motivation for investigating their growth by the commercially preferred metalorganic vapor phase epitaxy (MOVPE) method. Such nanowires can be grown using either a bottom-up approach using selective area epitaxy[8,9,10,11,12,13,14] or a top-down approach[15,16] in which nanowires with controlled aspect ratio are etched from a planar film before the re-growth of GaN/InGaN shell layers over the nanowires [4,16,17].

In contrast to planar layer growth, uniform InGaN growth on NWs is difficult because the three-dimensional (3D) growth mode leads to facet-dependent growth rates and indium nitride (InN) incorporation, leading to emission at multiple peak wavelengths [4,5,17,18,]. InGaN growth on pre-etched GaN NWs can be non-uniform for closely packed arrays[12,19], indicating a likely dependence of indium mole fraction incorporation on NW height and spacing.

In this paper we report the growth of InGaN layers on etched nanowire arrays after the crystallographic facets have been recovered by an initial GaN growth step. The emission properties of ensuing InGaN layers grown under different conditions are compared, in order to understand which parameters significantly influence the InGaN growth on the different facets available on the GaN NWs.

2 Experiment

2.1 Fabrication of template for MOVPE re-growth

NW arrays were created with a top-down approach[15] from a planar GaN/AlN/Si(111) wafer. A pattern of nickel dots, obtained by nanoimprint lithography and a lift-off process[20], was used to make a hard mask for a highly anisotropic Cl_2/Ar plasma etch to form the array of GaN NW cores. The pattern consisted of a hexagonal array of Ni dots of 600 nm diameter on a pitch of 2 μm and the plasma process resulted in NWs etched through the GaN and the AlN buffer layer into the Si(111) substrate.

Figure 1a shows a schematic of the cylindrical GaN NWs fabricated by this process. The starting GaN film was 1.5 μm thick with an additional 0.5 μm buffer layer of AlN used to manage the lattice strain within the GaN. Etching the NWs down into the Si substrate has the advantage that the etched Si surface can be converted to form a SiN_x selective growth mask, as seen in Fig. 1a, by an in-situ nitridation step prior to the GaN facet recovery step. This leads to GaN re-growth only on the etched cylindrical GaN cores, as shown in scanning electron microscope (SEM) images in Figures 1b and c.

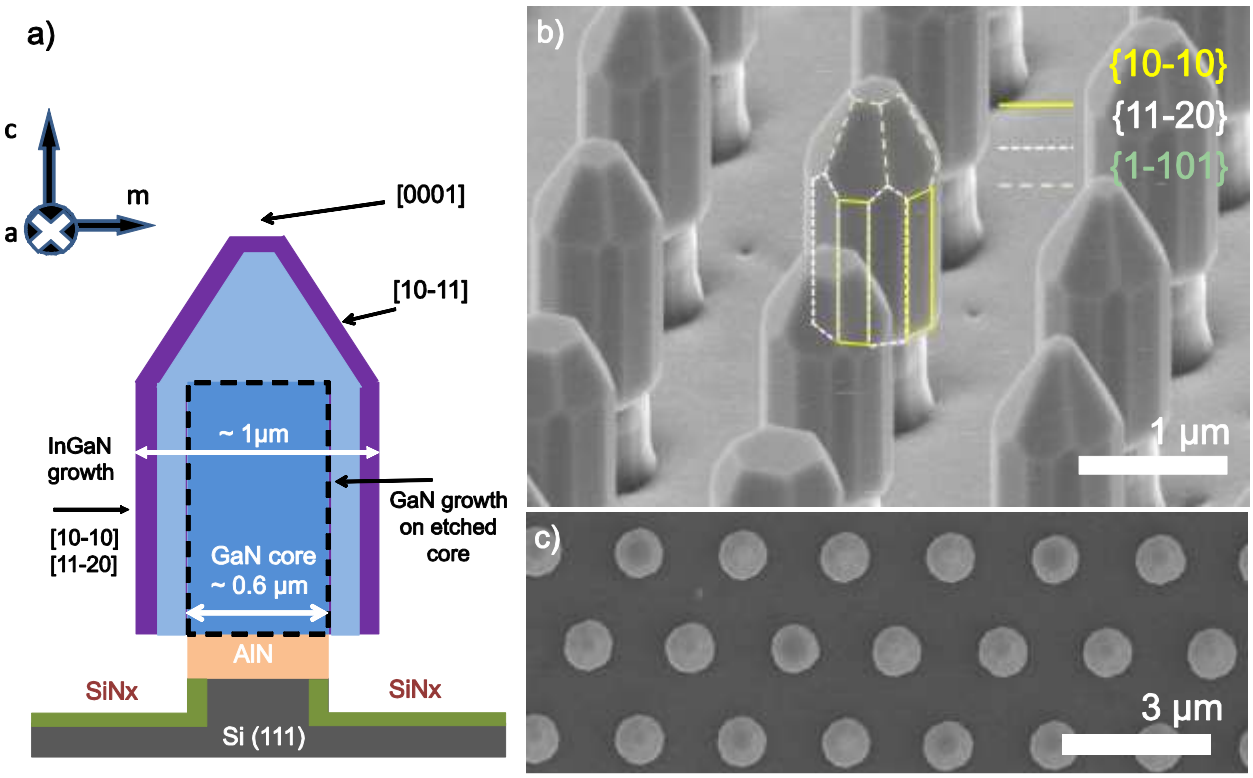

Figure 1. (color line) a) Schematic of the cross-section of a NW after GaN re-growth on the initial etched GaN core (not drawn at scale), b) tilted secondary-electron microscope (SEM) image of NWs with smooth non-polar facets and a small remaining flat c-plane , and c) plan view NW array with 2 µm pitch.

2.2 MOVPE re-growth

After the nitridation step, performed at 1050°C for 10 minutes and a short GaN nucleation step, a GaN facet recovery step was performed in the MOVPE reactor at 1060°C and 50 mbar for 5 minutes in order to obtain NWs with a regular, faceted shape, notably flat non-polar facets. These growth conditions were chosen to retain as many crystal planes as possible, in particular the {11-20} plane as shown in Figure. 1b. There was no GaN growth observed on the AlN buffer layer or on the Si between the NWs, the latter confirming the effectiveness of the SiN_x selective growth mask. In this work, for the subsequent InGaN layer growth, the reactor parameters determine the relative facet growth rates and the InN fraction incorporation on the respective facets. The TMIn and TMGa flows were kept constant across all the InGaN growths at 200 sccm and 9 sccm respectively. Three different InGaN growth conditions were considered with the

following parameters: 750°C at 300 mbar, 700°C at 300 mbar and 750°C at 100 mbar, on the same faceted GaN scaffold (Figure 1b), while all other parameters were unchanged. A growth time of 30 minutes was used in order to determine reliable growth rates from measurements of the thickness of the non-polar InGaN via SEM images, especially for structures grown at temperatures (700 - 800°C), that encourage InGaN desorption [21]; i.e. when the InN incorporation rate is low.

Figures 2a-c show secondary electron SEM images of the results of the three InGaN growth runs in which various crystal orientations are retained and can be identified: [0001], [1-101], [11-20] and [10-10]. In contrast to GaN re-growth, poor selectivity was obtained during InGaN deposition, as InGaN growth can be observed on the SiN_x surface in Figures 2a-c.

3 Characterization of Indium Gallium Nitride layers

The morphology of the InGaN layers were examined by taking planar secondary-electron microscope images of arrays of over 80 NWs for each image. Image processing software was used to attain statistically meaningful conclusions about the amount of growth after each of the growth steps. One sample was analyzed by TEM to examine the InGaN growth in more detail. Optical properties were assessed by cathodoluminescence (CL) hyperspectral imaging to determine emission characteristics, notably uniformity on the non-polar facets of interest and to estimate InN mole fraction.

The cylindrical GaN NWs retained a small *c*-plane (Figure 1b) after the short GaN facet recovery growth. With sufficient growth time the NW tips would form into a self-limiting pyramid shape[22,23,24], with the slower growing and more stable semi-polar {1-101} facets causing extinction of the faster growing planes[25] at convex surfaces. Similarly extinction of the faster growing *a*-planes will occur on the vertical sidewalls of the NWs, leaving

structures of hexagonal cross section, terminated by *m*-planes. Since InGaN growth on the *a*-planes formed part of this study, the duration of the GaN facet recovery growth was kept short, with the consequence the NWs had a residual [0001] plane.

In contrast to GaN re-growth, the InGaN growth in Figures 2a-c show increased surface roughness on the c-plane, indicating a layer of unstrained indium rich growth [26,27].

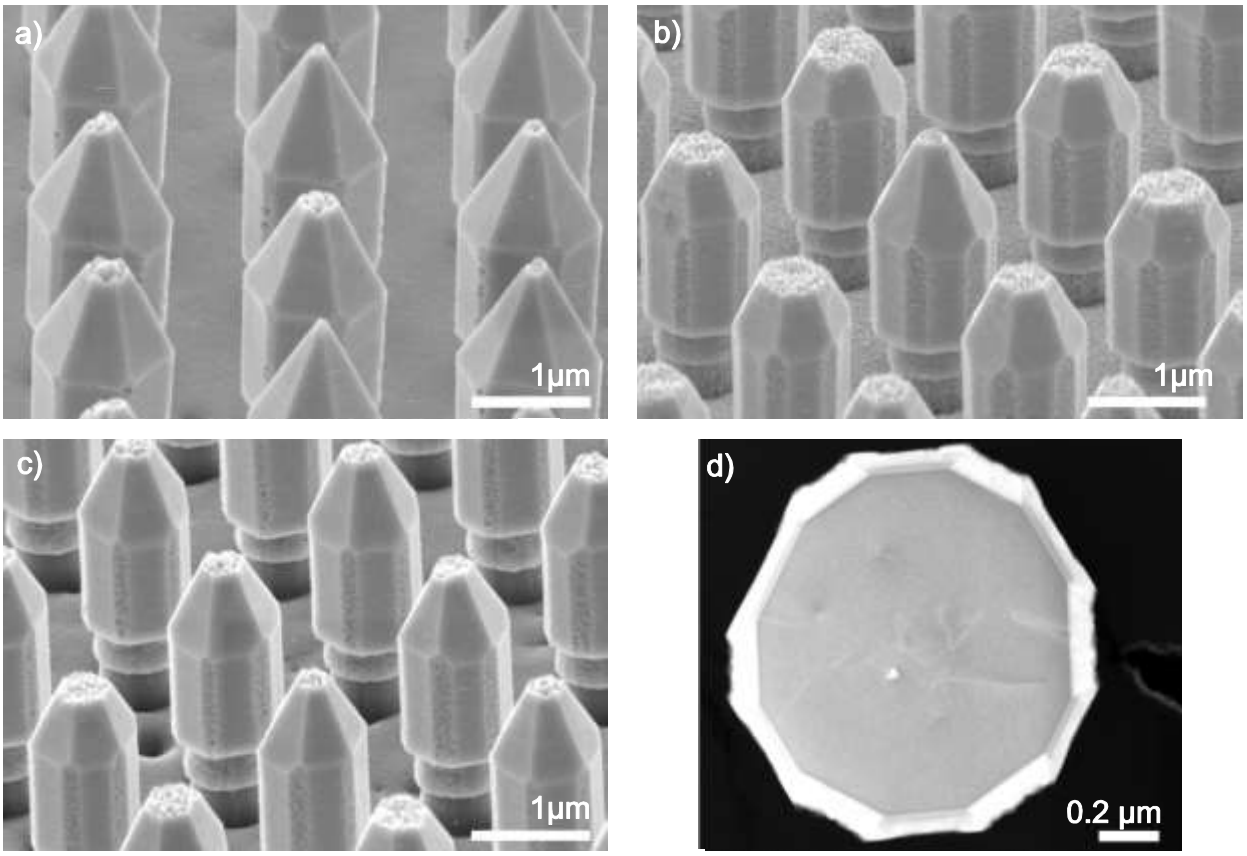

Figure 2. NWs after InGaN layer growth a) 750°C 300 mbar shows a small remaining (0001) plane with nano pyramids, {10-10} *m*-planes, and minimized {11-20} facets, b) 700°C and 300 mbar results in an increase in roughness on all planes, c) 750°C and 100 mbar shows nano pyramids on the (0001) *c*-plane, *m*-planes more similar to the high temperature growth, and high roughness on the {11-20} *a*-plane, more similar to the low temperature sample d) TEM lamella of sample obtained at 700°C and 300 mbar shows different lateral growth thickness and length between the *a*- and *m*-planes.

On the macro scale the different crystal planes are known to have different relative growth rates[25] determined by growth parameters[28,29] and potentially result in different InN mole fractions on the crystal planes, as shown by previous work[4,17,24]. However it is unclear if the growth

dynamics on wire-shaped nanostructures will be the same. For example, the dimensions of the facets could be less than the surface diffusion length of Ga or In, and pseudomorphic strain at the interfaces between planes may be lower. Both factors could influence InN fraction. On the NWs used in this work the {11-20} and {10-10} facets originating from the template are retained after the InGaN growth.

The SEM images in Figure 2 show that changes in growth parameters and the long growth time had a clear impact on the morphology of the crystal facets, in particular the relative growth rates of the facets[29], which in turn are related to the surface energies of the various planes [30,31]. The growth rates shown in Table 1 were obtained from the increase in equivalent diameter, as determined from the image analysis software.

Figures 2 a-c show that temperature and pressure have the dominant impact on the *a*- and the *m*-planes, as far as determining the relative size and their surface roughness. Use of a high temperature has reduced the proportion of *a*- to *m*- plane observable compared with the facetted GaN core because the temperature increases the relative growth rate of the of the {11-20} facet, and thus this sample has only a small residual {11-20} surface. Furthermore there is a tendency for indium atoms to stick at the apices between planes, which create more irregular surfaces where the adatoms can be captured, leading to non-uniform wavelength light emission[17]. At 700°C and 300 mbar the relative growth rates of the non-polar planes are closer in value, causing a different *m*- to *a*-plane growth rate ratio. Also the indium desorption and diffusion length are both lower than at 750°C, making the incorporation of more indium atoms possible. As the indium atom diffusion length becomes comparable to the distance between binding sites on the sidewalls, there is a visible roughening of the sidewalls. In Ref. [32] it is indicated that a statistical roughening of the surfaces can be expected on the (0001) and (000-1) surfaces, if the diffusion

length becomes shorter than the mean distance between binding sites. Surface roughening encourages local fluctuations in the captured InN mole fraction on the non-polar planes. Reduction of the growth pressure to 100 mbar, while keeping the temperature at 750°C, had the effect of reducing the InGaN growth rates of both the *m*- and *a*- planes, to an average rate of ~1.3 nm/min, as the increase in the size of the overall NW is smaller. The presence of residual {11-20} *a*-plane on this sample indicates that the relative growth rates of the *m*- to *a*-plane, differs to the other sample grown at 750°C. Note the reduction in growth pressure tends to increase indium surface diffusion[33], because low pressure reduces the indium atom collision probability. In support of this, the roughness has diminished on the {10-10} *m*-plane in Figure 2c compared to Figure 2b, while the {11-20} *a*-plane is still very rough even at low growth rate. This result indicates the *a*-plane growth conditions need further optimization for it to be useful as a stable crystal facet on NW structures.

Table 1 lists the combined average growth rates of the non-polar planes planes obtained from the image analysis method for the three samples used in this work. To compare growth rates of the SEM and get an assessment of separate *a*- and *m*-plane contributions, a plan-view, i.e. perpendicular to the *c*-axis, TEM sample of a single NW was prepared. The TEM measurements were determined from a single NW, while the SEM measurements were determined from a statistical set, on different calibrated equipment, which accounts for the difference in diameter. Image processing for the TEM data was done in a similar manner to the SEM data. The TEM ratio of lengths of *m*- to *a*-plane is 1.68, a ratio that can be controlled by the template used, the growth time and growth parameters. The growth rate was determined at 2.3 nm/min on the *m*-plane, and 3.1nm/min on the *a*-plane, making the ratio of *m*-plane to *a*-plane growth rates 0.74, for 700°C and 300 mbar.

Table 1. Comparison of growth rates corresponding to the three InGaN growths.

Sample	*Technique*	*Diameter (Std dev) [nm]*	*Radius increase -layer thickness- [nm]*	*Average growth rate of non-polar facets [nm/min]*
GaN re-growth	SEM	923 (13)		
750°C 300 mbar	SEM	1094 (15)	85.4	2.8
750°C 100 mbar	SEM	999 (13)	37.9	1.3
700°C 300 mbar	SEM	1079 (15)	78.0	2.6
	TEM	1265	84.6	2.8

In examining the TEM lamella in Figure 2d, it is worth mentioning that the GaN facets grow seamlessly at the etched interfaces, because there is no difference in contrast between the core and regrown facets. However the InGaN shell is immediately distinguishable. Furthermore the different contrast at the *m*-plane interfaces show a change in InN mole fraction after an initial layer thickness (~20nm) is achieved, a behavior related to a change in strain [27,34].

Cathodoluminescence hyperspectral imaging was used to determine the photon emission characteristics of the thick InGaN layers formed on the different facets of the NWs and to estimate, for an unstrained layer, the InN mole fraction, using the emission energy as a function of composition[35,36]. The estimated InGaN layer widths were sufficiently large that the quantum confinement effect is negligible, for the photon emission energy to provide a good estimate of the bandgap, hence composition. Hyperspectral CL measures a full spectrum from each point on the surface scanned by the electron beam. In this work, CL spectra were collected at room temperature for a beam energy of 5 keV and step size of 25 nm, to create 200×200 pixel maps. Figures 3a-c show real color images that have been determined from the chromaticity

coordinates of the collected spectra and thereby illustrate the impact of the growth conditions on the obtained InGaN layer.

The CL maps in Figures 3a-c show each facet in a different color, caused by different InGaN composition and facet dependent InN fraction incorporation rates. Corresponding spectra extracted from the same hyperspectral datasets are shown in Figure 3d for the crystal planes considered. The spectra were taken from representative areas averaging 4×4 pixels from each facet. For all samples the residual (0001) plane emits in the range of 2.05 - 2.28 eV, with different relative intensities from sample to sample.

On the sample grown at 750°C and 300 mbar (Figure 3a), the {10-10} *m*-plane displays emission mainly at 2.83 eV. Compared to the other samples the residual {11-20} plane, is much reduced in size due to its faster growth rate relative to {10-10} planes, and has an emission centered on 2.65 eV, with a high energy shoulder at 2.83eV due to simultaneous emission from the nearby m-planes.

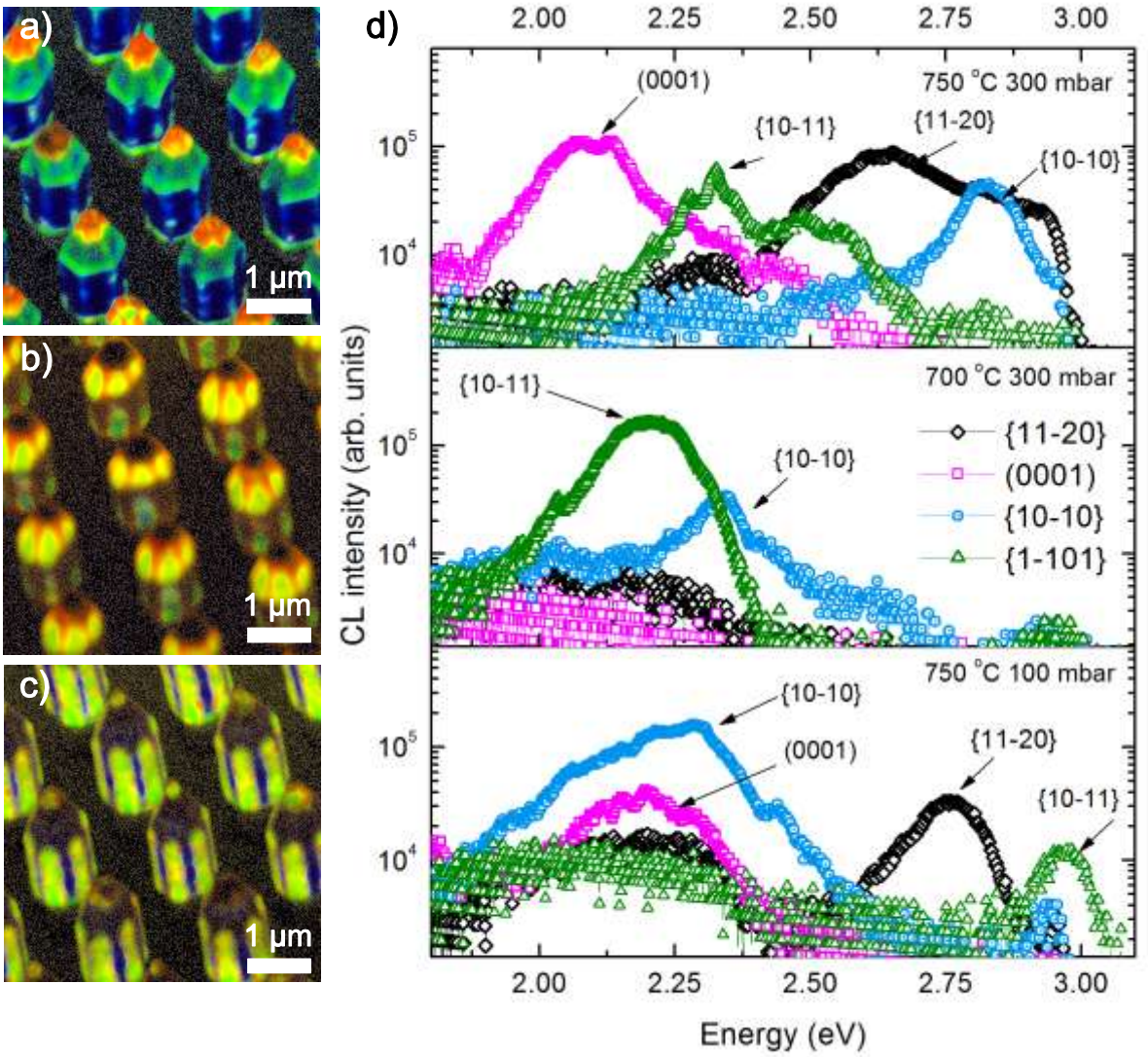

Figure 3. (color online) Real color images and corresponding CL spectra a) 750°C 300 mbar with dissimilar emission from every facet , b) 700°C 300 mbar sample with main emission from the {1-101} facets, c) 750°C 100 mbar with high intensity emission from the m-plane facets, d) spectra collected from a representative area of 4x4 pixels on each facet.

The {1-101} semi-polar facets exhibit two emission peaks, changing emission color from the middle of the facet towards the edge. The facet center emits at 2.49 eV, whereas the most intense emission originates from the apices, at 2.33 eV. The latter is caused by either a reduction in strain at the apices, or by increased indium atom incorporation in the localized regions.

For the 700°C InGaN growth, no emission was identified on the rough a-plane, possibly due to surface states introduced by roughening, acting as paths for nonradiative recombination[37] at high indium concentrations[38]. There were areas with emission peaks from the {10-10} facets at 2.35eV, 2.62 eV and a weak emission at 2.95eV. This is probably caused by the indium fraction incorporating on the more irregular surfaces of this sample, while the 2.95eV may originate from a fraction deeper in the facet, grown first on the recovered GaN facets and likely strained, as is shown in the TEM image (see Figure 2d). The dominant emission originates on the {1-101} semi-polar facets and is centered at 2.20 eV. Overall the decrease in temperature resulted in red shifted emission from all the facets due to higher indium incorporation on all surfaces as a consequence of reduced desorption rate.

Figure 3c for the growth at 750°C and 100 mbar shows a broad emission around 2.29 eV which originates on the {10-10} facets, with additional peaks at 2.43eV and 2.95 eV, the later related to a strained layer as well. The {11-20} planes have a distinct emission at 2.75 eV. The {1-101} semi-polar planes are emitting at 2.97 eV with a low intensity peak, and this emission is relatively quenched.

4 Discussion

The results confirm that the InGaN growth rates and InN mole fraction are strongly dependent on the crystal plane orientation and the growth parameters. The growth parameters can be used to alter the relative growth rates between the *m*- and *a*-plane, leading to different extents of the {11-20} facet, when starting from identical faceted GaN NWs. Roughness on the crystal facets, caused by either unstrained InGaN growth resulting from a 3D growth mode or rapid InN incorporation related to the short diffusion length of In, causes local variations of the indium mole fraction and the likely widening of the CL emission spectra.

The decrease of the growth temperature from 750°C to 700°C led to an increase of the InN mole fraction, estimated by CL to be from 13% to 24% on the {10-10} plane, and from 20-25% to 25-30% on the {1-101} plane. The difference in contrast along the [10-10] direction observed in TEM for the 700°C sample (see Figure 2d), from a dark InGaN layer to a brighter one, indicate an increase of the InN mole fraction [39] after the initial pseudomorphic InGaN layer exceeds the critical layer thickness. In addition to local variations of InN fraction, this can explain the double peak nature of the CL emission spectra.

Table 2. Correlation of observed CL peak emission energy and InN mole fraction, as determined by the composition dependence of the bandgap.

Sample	*750°C 300 mbar*			*700°C 300 mbar*			*750°C 100 mbar*		
Plane	{10-10}	{11-20}	{1-101}	{10-10}	{11-20}	{1-101}	{10-10}	{11-20}	{1-101}
Peak (eV)	2.83	2.65	2.33 -2.49	2.35-2.95	-	2.20	2.29-2.95	2.76	2.97
InN (%)	13	17	25 - 20	24 – 14*	-	27	25-14*	15	13*

*values determined using a strained InGaN model[40]

As can be seen in Table 2, at 300 mbar the average InN mole fraction was found to be higher on the {11-20} *a*-plane (17 %), and the {1-101} plane (20-25%), than for the {10-10} *m*-plane, where the indium composition is generally 13%. This result indicates that, despite the thick shell allowing for unstrained growth, this set of growth conditions still limits the incorporation efficiency.

The reduction of pressure from 300 mbar to 100 mbar has had a large impact on the growth of all crystal planes. Use of 100 mbar pressure and 750°C growth temperature caused a change in the InN mole fraction between the non-polar planes; specifically a greater indium composition resulted on the *m*-planes (25%) than on the *a*-planes (15%) or on the semi-polar {1-101} planes (10% or more accurately 13%, if the unstrained InGaN model[40] is considered). This was unexpected as the growth rate was low on this sample, (see Table 1), and both low pressure and high temperature cause high diffusion lengths for the indium atoms. However from work on

c-plane[41,42] and *a*-plane[43] planar thin films, it was found that low pressure can increase indium incorporation. This was suggested to be caused by the suppression of indium desorption with enhanced gas mass transfer rates of precursor species through the boundary layer[41], as the diffusion in gases varies inversely proportional with pressure[44]. The measurements reported here show that even at low growth rate, a high InN incorporation efficiency on the *m*-plane facets can be achieved with low pressure, to achieve high InN mole fraction InGaN layers being grown.

5 Conclusion

A GaN template of vertically aligned nanowires with (0001), {10-10}, {11-20} and {1-101} facets was fabricated to study the effect of pressure and temperature on the growth rates and emission characteristics of thick (~ 40-80 nm) InGaN layers for core-shell light-emitting devices. The growth rates of the non-polar planes were determined from SEM images and correlated with TEM analysis. The InGaN growth rates on the non-polar planes varied from 1.3 to 2.8 nm/min, depending on growth temperature and pressure. Each growth led to a different set of emission peaks, i.e. a different InN fraction was incorporated on each facet. The InN mole fraction incorporated on each crystal facet was estimated by comparing the emission peak measured by CL hyperspectral imaging with previously published data[35,36,40]. The study revealed that the reduction of pressure to 100 mbar led to a more efficient InN mole fraction integration on the {10-10} m-plane, increasing it from 13% to 25%. This may be used to obtain green-yellow core-shell LEDs with a high InN mole fraction based on emission from the {10-10} m-planes. The study has shown how growth parameters can control the relative crystal facet growth rates and InN mole fraction. This understanding can guide design for core-shell LEDs.

Acknowledgements

The authors would like to thank OSRAM Opto Semiconductors GmbH for the provision of the GaN/silicon templates and acknowledge financial support from the European Union (FP7 Contract No.: 228999, “SMASH”) and the EPSRC, UK via Grant No. EP/I012591/1 “Lighting the Future.” We gratefully acknowledge the Leeds EPSRC Nanoscience and Nanotechnology Facility (grant EP/K023853/1) and Dr. Michael Ward for the focused ion beam (FIB) sample preparation.

[1] Romanov, A. E., Baker, T. J., Nakamura, S.., Speck, J. S., "Strain-induced polarization in wurtzite III-nitride semipolar layers," J. Appl. Phys. **100**(2), 023522 (2006).

[2] Farrell, R. M., Young, E. C., Wu, F., DenBaars, S. P.., Speck, J. S., "Materials and growth issues for high-performance nonpolar and semipolar light-emitting devices," Semicond. Sci. Technol. **27**(2), 024001 (2012).

[3] Hong, Y. J., Lee, C.-H., Yoon, A., Kim, M., Seong, H.-K., Chung, H. J., Sone, C., Park, Y. J.., Yi, G.-C., "Visible-color-tunable light-emitting diodes.," Adv. Mater. **23**(29), 3284–3288 (2011).

[4] Chang, J.-R., Chang, S.-P., Li, Y.-J., Cheng, Y.-J., Sou, K.-P., Huang, J.-K., Kuo, H.-C.., Chang, C.-Y., "Fabrication and luminescent properties of core-shell InGaN/GaN multiple quantum wells on GaN nanopillars," Appl. Phys. Lett. **100**(26), 261103 (2012).

[5] Yeh, T.-W., Lin, Y.-T., Stewart, L. S., Dapkus, P. D., Sarkissian, R., O'Brien, J. D., Ahn, B.., Nutt, S. R., "InGaN/GaN multiple quantum wells grown on nonpolar facets of vertical GaN nanorod arrays.," Nano Lett. **12**(6), 3257–3262 (2012).

[6] Kishino, K., Sekiguchi, H.., Kikuchi, A., "Improved Ti-mask selective-area growth (SAG) by rf-plasma-assisted molecular beam epitaxy demonstrating extremely uniform GaN nanocolumn arrays," J. Cryst. Growth **311**(7), 2063–2068 (2009).

[7] Waag, A., Wang, X., Fündling, S., Ledig, J., Erenburg, M., Neumann, R., Al Suleiman, M., Merzsch, S., Wei, J., et al., "The nanorod approach: GaN NanoLEDs for solid state lighting," Phys. Status Solidi **8**(7-8), 2296–2301 (2011).

[8] Hersee, S. D., Sun, X.., Wang, X., "The Controlled Growth of GaN Nanowires," Nano Lett. **6**(8), 1808–1811 (2006).

[9] Tang, T., Lin, C., Chen, Y., Shiao, W., Chang, W., Liao, C., Shen, K., Yang, C., Member, S., et al., "Nitride Nanocolumns for the Development of Light-Emitting Diode," IEEE Trans. Electron Devices **57**(1), 71–78 (2010).

[10] Bergbauer, W., Strassburg, M., Kolper, C., Linder, N., Roder, C., Lähnemann, J., Trampert, A., Fundling, S., Li, S. F., et al., "Continuous-flux MOVPE growth of position-controlled N-face GaN nanorods and embedded InGaN quantum wells.," Nanotechnology **21**(30), 305201 (2010).

[11] Tomioka, K., Tanaka, T., Hara, S., Hiruma, K.., Fukui, T., "III – V Nanowires on Si Substrate : Selective-Area Growth and Device Applications," IEEE J. Sel. Top. Quantum Electron. **17**(4), 1112–1129 (2011).

[12] Liao, C.-H., Chang, W.-M., Yao, Y.-F., Chen, H.-T., Su, C.-Y., Chen, C.-Y., Hsieh, C., Chen, H.-S., Tu, C.-G., et al., "Cross-sectional sizes and emission wavelengths of

regularly patterned GaN and core-shell InGaN/GaN quantum-well nanorod arrays," J. Appl. Phys. **113**(5), 054315 (2013).

[13] Choi, K., Arita, M.., Arakawa, Y., "Selective-area growth of thin GaN nanowires by MOCVD," J. Cryst. Growth **357**, 58–61, Elsevier (2012).

[14] Coulon, P.-M., Alloing, B., Brändli, V., Lefebvre, D., Chenot, S.., Zúñiga-Pérez, J., "Selective area growth of Ga-polar GaN nanowire arrays by continuous-flow MOVPE: A systematic study on the effect of growth conditions on the array properties," Phys. Status Solidi **252**(5), 1096–1103 (2015).

[15] Shields, P., Hugues, M., Zúñiga-Pérez, J., Cooke, M., Dineen, M., Wang, W., Causa, F.., Allsopp, D., "Fabrication and properties of etched GaN nanorods," Phys. Status Solidi **9**(3-4), 631–634 (2012).

[16] Krylyuk, S., Paramanik, D., King, M., Motayed, A., Ha, J.-Y., Bonevich, J. E., Talin, A.., Davydov, A. V., "Large-area GaN n-core/p-shell arrays fabricated using top-down etching and selective epitaxial overgrowth," Appl. Phys. Lett. **101**(24), 241119 (2012).

[17] Le Boulbar, E. D., Gîrgel, I., Lewins, C. J., Edwards, P. R., Martin, R. W., Šatka, A., Allsopp, D. W. E.., Shields, P. A., "Facet recovery and light emission from GaN/InGaN/GaN core-shell structures grown by metal organic vapour phase epitaxy on etched GaN nanorod arrays," J. Appl. Phys. **114**(9), 094302 (2013).

[18] Riley, J. R., Padalkar, S., Li, Q., Lu, P., Koleske, D. D., Wierer, J. J., Wang, G. T.., Lauhon, L. J., "Three-Dimensional Mapping of Quantum Wells in a GaN / InGaN," Nano Lett. **13**, 4317–4325 (2013).

[19] Lewins, C. J., Le Boulbar, E. D., Lis, S. M., Edwards, P. R., Martin, R. W., Shields, P. a.., Allsopp, D. W. E., "Strong photonic crystal behavior in regular arrays of core-shell and quantum disc InGaN/GaN nanorod light-emitting diodes," J. Appl. Phys. **116**(4), 044305 (2014).

[20] Shields, P. a.., Allsopp, D. W. E., "Nanoimprint lithography resist profile inversion for lift-off applications," Microelectron. Eng. **88**(9), 3011–3014, Elsevier B.V. (2011).

[21] Schenk, H. P. D., de Mierry, P., Laügt, M., Omnès, F., Leroux, M., Beaumont, B.., Gibart, P., "Indium incorporation above 800°C during metalorganic vapor phase epitaxy of InGaN," Appl. Phys. Lett. **75**(17), 2587 (1999).

[22] Fichtenbaum, N. A., Neufeld, C. J., Schaake, C., Wu, Y., Wong, M. H., Grundmann, M., Keller, S., DenBaars, S. P., Speck, J. S., et al., "Metalorganic Chemical Vapor Deposition Regrowth of InGaN and GaN on N-polar Pillar and Stripe Nanostructures," Jpn. J. Appl. Phys. **46**(No. 10), L230–L233 (2007).

[23] Liu, C., Šatka, A., Jagadamma, L. K., Edwards, P. R., Allsopp, D., Martin, R. W., Shields, P., Kovac, J., Uherek, F., et al., "Light Emission from InGaN Quantum Wells Grown on the Facets of Closely Spaced GaN Nano-Pyramids Formed by Nano-Imprinting," Appl. Phys. Express **2**(12), 121002 (2009).

[24] Miao, C., Honda, Y., Yamaguchi, M.., Amano, H., "Growth of InGaN/GaN multiple quantum wells on size-controllable nanopyramid arrays," Jpn. J. Appl. Phys. **53**(030306) (2014).

[25] Leung, B., Sun, Q., Yerino, C. D., Han, J.., Coltrin, M. E., "Using the kinetic Wulff plot to design and control nonpolar and semipolar GaN heteroepitaxy," Semicond. Sci. Technol. **27**(2), 024005 (2012).

[26] Pereira, S., Correia, M. R., Pereira, E., Trager-Cowan, C., Sweeney, F., O'Donnell, K. P., Alves, E., Franco, N.., Sequeira, a. D., "Structural and optical properties of InGaN/GaN layers close to the critical layer thickness," Appl. Phys. Lett. **81**(7), 1207 (2002).

[27] Leyer, M., Stellmach, J., Meissner, C., Pristovsek, M.., Kneissl, M., "The critical thickness of InGaN on (0001)GaN," J. Cryst. Growth **310**(23), 4913–4915 (2008).

[28] Bryant, B. N., Hirai, A., Young, E. C., Nakamura, S.., Speck, J. S., "Quasi-equilibrium crystal shapes and kinetic Wulff plots for gallium nitride grown by hydride vapor phase epitaxy," J. Cryst. Growth **369**, 14–20, Elsevier (2013).

[29] Sun, Q., Yerino, C. D., Ko, T. S., Cho, Y. S., Lee, I.-H., Han, J.., Coltrin, M. E., "Understanding nonpolar GaN growth through kinetic Wulff plots," J. Appl. Phys. **104**(9), 093523 (2008).

[30] Northrup, J. E.., Neugebauer, J., "Theory of GaN (10-10) and (11-20) surfaces," Phys. Rev. B **53**(16), 477–480 (1996).

[31] Neugebauer, J., "Ab initio Analysis of Surface Structure and Adatom Kinetics of Group-III Nitrides," Phys. Status Solidi **227**(1), 93–114 (2001).

[32] Zywietz, T., Neugebauer, J.., Scheffler, M., "Adatom diffusion at GaN (0001) and (000$\bar{1}$) surfaces," Appl. Phys. Lett. **73**(4), 487 (1998).

[33] Cho, H. K., Lee, K. H., Kim, S. W., Park, K. S., Cho, Y.-H.., Lee, J. H., "Influence of growth temperature and reactor pressure on microstructural and optical properties of InAlGaN quaternary epilayers," J. Cryst. Growth **267**(1-2), 67–73 (2004).

[34] Pristovsek, M., Stellmach, J., Leyer, M.., Kneissl, M., "Growth mode of InGaN on GaN (0001) in MOVPE," Phys. Status Solidi **6**(S2), S565–S569 (2009).

[35] Davydov, V. Y., Klochikhin, A. a., Emtsev, V. V., Kurdyukov, D. a., Ivanov, S. V., Vekshin, V. a., Bechstedt, F., Furthmuller, J., Aderhold, J., et al., "Band Gap of Hexagonal InN and InGaN Alloys," Phys. Status Solidi **234**(3), 787–795 (2002).

[36] O'Donnell, K. P., Fernandez-Torrente, I., Edwards, P. .., Martin, R. ., "The composition dependence of the Inx Ga1−x N bandgap," J. Cryst. Growth **269**(1), 100–105 (2004).

[37] Hahn, C., Cordones, A. A., Andrews, S. C., Gao, H., Fu, A., Leone, S. R.., Yang, P., "Effect of Thermal Annealing in Ammonia on the Properties of InGaN Nanowires with Different Indium Concentrations," J. Phys. Chem. C **7**(117), 3627–3634 (2013).

[38] Langer, T., Kruse, A., Ketzer, F. A., Schwiegel, A., Hoffmann, L., Jonen, H., Bremers, H., Rossow, U.., Hangleiter, A., "Origin of the 'green gap': Increasing nonroadiative recombination in indium-rich GaInN/GaN quantum well structures," Phys. Status Solidi 8 **8**(7-8), 2170–2172 (2011).

[39] Li, Q.., Wang, G. T., "Strain influenced indium composition distribution in GaN/InGaN core-shell nanowires," Appl. Phys. Lett. **97**(18), 181107 (2010).

[40] Orsal, G., El Gmili, Y., Fressengeas, N., Streque, J., Djerboub, R., Moudakir, T., Sundaram, S., Ougazzaden, a.., Salvestrini, J. P., "Bandgap energy bowing parameter of strained and relaxed InGaN layers," Opt. Mater. Express **4**(5), 1030 (2014).

[41] Kim, D., Moon, Y., Song, K., Lee, I.., Park, S., "Effect of Growth Pressure on Indium Incorporation During the Growth of InGaN by MOCVD," J. Electron. Mater. **30**(2), 99–102 (2001).

[42] Oliver, R. A., Kappers, M. J., Humphreys, C. J.., Briggs, G. A. D., "The influence of ammonia on the growth mode in InGaN/GaN heteroepitaxy," J. Cryst. Growth **272**(1-4), 393–399 (2004).

[43] Song, K.-M.., Park, J., "Effects of the growth pressure of a -plane InGaN/GaN multi-quantum wells on the optical performance of light-emitting diodes," Semicond. Sci. Technol. **28**(1), 015010 (2013).

[44] Ohring, M., Materials Science of Thin Films Deposition and Structure, 2nd Ed., p296, Academic Press, London (1992).

Ionut Girgel is a PhD student in the Department of Electronic and Electrical Engineering at the University of Bath. He received his M.Sc in Condensed Matter Physics and his B.Sc in Applied Physics from Ovidius University of Constanta, Romania. His PhD research is in the area of core-shell InGaN/GaN devices.

Paul Edwards is a Senior Research Fellow in the Department of Physics at the University of Strathclyde. He received his B.Sc. and Ph.D. degrees from Imperial College London and the University of Durham in 1995 and 1999, respectively. He has authored 120 journal and conference papers on the optical and electron beam characterization of compound semiconductors.

Emmanuel Le Boulbar is a research officer in the Department of Mechanical Engineering at the University of Bath. He received his D.Phil. degree in material science from the University of Orleans, France, in 2010. His current research interests include the growth and fabrication of III-nitride nanostructures for optoelectronic and water-splitting applications.

Pierre-Marie Coulon is a research assistant in the Department of Electronic and Electrical Engineering at the University of Bath. He received M.Phys. and D.Phil. degrees in Physics from the University of Nice Sophia-Antipolis in 2010 and 2014 respectively. His research interest is in the growth and characterization of III-nitride devices mainly for optoelectronic applications, with a particular focus on growth mechanisms within nanostructures.

Suman-Lata Sahonta obtained her PhD in electron beam analysis of ultra-wide band gap nitride materials at the University of Bristol. She is currently a postdoctoral fellow in the Cambridge Centre for Gallium Nitride at the University of Cambridge.

Duncan Allsopp received the B.Sc. degree in physics and the M.Sc. and Ph.D. degrees from the University of Sheffield, Sheffield, U.K., in 1971, 1974, and 1977, respectively. From 1977 to 1979, he was with Ferranti Electronics Ltd., Oldham, U.K., the University of Manchester Institute of Science and Technology, Manchester, U.K., where he is involved in research on defects in semiconductors, from 1979 to 1984, and the British Telecom Research Laboratories, Martlesham Heath, Suffolk, U.K., from 1984 to 1986. In 1986, he joined the University of York, York, U.K., where he established a group researching photonic devices. Since 1999, he has been at University of Bath, Bath, U.K., where he leads the III-Nitride Research Group.

Robert Martin is Professor of Experimental Physics in the Department of Physics at Strathclyde University in Glasgow, UK. He received MA and D.Phil. degrees in Physics from the University of Oxford in 1988 and 1992 respectively. He has published over 240 papers on the properties of semiconductor and other advanced materials, in particular the iii-nitrides. He is a Fellow of the Institute of Physics.

Colin Humphreys is Professor and Director of Research in the Department of Materials Science and Metallurgy at the University of Cambridge. He has published over 600 papers on electron microscopy, gallium nitride and other materials and device structures. He is a Fellow of the Royal Society and of the Royal Academy of Engineering.

Philip Shields is a Lecturer (Assistant Professor) in the Department of Electronic and Electrical Engineering at the University of Bath. He received his M.Phys and D.Phil. degrees in physics from the University of Oxford, U.K, in 1997 and 2001 respectively. His research interest is in the growth and fabrication of III-nitride devices mainly for optoelectronic applications, with a particular focus on the use of nanostructures to improve device performance.

Caption List

Figure 1 a) Schematic of cross-section NW after GaN re-growth on the initial etched GaN core (not drawn at scale), b) tilted secondary-electron SEM image of NWs with smooth non-polar facets and a small remaining flat c-plane , and c) plan view NW array with 2 µm pitch.

Figure 2 NWs after InGaN layer growth a) 750°C 300 mbar shows a small remaining (0001) plane with Nano pyramids, {10-10} m-planes, and minimized {11-20} facets, b) 700°C and 300 mbar illustrates an increase in roughness on all planes, c) 750°C and 100 mbar shows nano pyramids on the (0001) c-plane, m-planes more similar to the high temperature growth, and high roughness on the {11-20} a-plane, more similar to the low temperature sample d) TEM lamella of sample obtained at 700°C and 300 mbar shows different lateral growth thickness and length between the *a*- and *m*-planes.

Figure 3 Real color images and corresponding CL spectra a) 750°C 300 mbar with dissimilar emission from every facet , b) 700°C 300 mbar sample with main emission from {1-101} facet , c) 750°C 100 mbar with high intensity emission from m-plane facet, d) spectra collected from a representative area of 4x4 pixels on each facet.

Table 1 Comparison of growth rates corresponding to the three InGaN growths.

Table 2 Correlation of observed CL peak emission energy and InN mole fraction, as determined by the composition dependence of the bandgap.